Chemical Engineering Journal 156 (2010) 278–285

Contents lists available at ScienceDirect

Chemical Engineering Journal

journal homepage: www.elsevier.com/locate/cej

Response surface optimization of photocatalytic process for degradation of Congo Red using H-titanate nanofiber catalyst

Meng Nan Chong[a,b], H.Y. Zhu[c], Bo Jin[a,b,d,*]

[a] School of Chemical Engineering, The University of Adelaide, Adelaide, SA 5005, Australia
[b] School of Earth and Environmental Sciences, The University of Adelaide, Adelaide, SA 5005, Australia
[c] School of Physical and Chemical Sciences, Queensland University of Technology, Brisbane, QLD 4001, Australia
[d] Australian Water Quality Centre, Bolivar, SA Water Corporation, SA 5110, Australia

ARTICLE INFO

Article history:
Received 18 May 2009
Received in revised form 6 October 2009
Accepted 6 October 2009

Keywords:
TiO_2
Nanofibers
Congo Red
Response surface analysis
Optimization
Factor interaction
Taguchi method

ABSTRACT

In this study, a new generation H-titanate nanofiber catalyst (TNC) with long fibril morphology and surface covered anatase titanium dioxide (TiO_2) crystals of 10–20 nm was used as the photocatalyst for improved photoactivity, mass transfer resistance and downstream separation. The combined Taguchi method and response surface analysis (RSA) were employed to evaluate the effects of key operational factors of TNC loading, pH, aeration rate and initial Congo Red (CR) concentration on the performances of TNC in an annular slurry photoreactor (ASP). The average CR photocatalytic degradation rate (mg dm^{-3} min^{-1}) was estimated and applied as the response outputs of the L_9 $(3)^4$ Taguchi orthogonal array. Results from the RSA interpretations revealed that pH, initial CR concentration and aeration rate were the significant factors, while TNC loading appears to be the least significant factor. On contrary, positive interactions of TNC loading were observed when being coupled with pH and aeration rate. Other interactions of the operation factors were also determined using statistical analysis. A natural logarithmic modified regression equation was developed from multiple regression analysis for response surface modelling. This model predicted that the average photocatalytic degradation rate of CR was 0.1576 mg dm^3 min^{-1} under the optimal conditions. A subsequent verification experiment showed a photocatalytic degradation rate of 0.1563 ± 0.0282 mg dm^{-3} min^{-1}, which is in good agreement with the model predicted value. This proved the applicability of the developed model as a reliable design and modelling tool for scaling up the photocatalytic reactor process.

1. Introduction

Development of advanced water treatment technologies with high efficacy, low cost, and "*zero*" waste outputs are at the forefront of R&D fields owing to the increasingly stringent environmental pressure [1–3]. Among the currently available water abatement technologies, heterogeneous titanium dioxide (TiO_2) photocatalytic treatment processes have emerged as a promising candidate for sustainable removal of recalcitrant organic pollutants without generation of any secondary pollution [3–7]. This is solely attributed to the reactive oxygen species generated on the surface of the TiO_2 particles [8]. These oxidative species (i.e. $OH^{\bullet}$, $O_2^{\bullet -}$, H_2O_2) can subsequently degrade the organic pollutants, eventually leading to a complete mineralization with innocuous of water and carbon dioxide molecules as the final by-products [1–7].

However, there are a few technical challenges which make this TiO_2 technology unviable as an industrial treatment process. One of the more prominent issues is the difficulty and high cost for downstream process to separate the TiO_2 particles after the water treatment process [9,10]. The TiO_2 particles exhibit excellent quantum properties (i.e. efficient charge separation, opaqueness and light refractive index) when the particles size lies in the nanometer range [11]. Increasing the particle size of TiO_2 will leads to serious deterioration in photoactivity, although such shift in particle size (towards bulk characteristics) promises ease of recovery. This has lead to numerous efforts to immobilize the nano-size TiO_2 particles onto larger inert substrates where the quantum properties can be conserved and effectively utilized [1,10,12,13]. In previous study, a new nanofiber TiO_2 photocatalyst was developed in which anatase crystals of 10–20 nm was successfully deposited on titanate fibril of 40–100 nm thickness and length up to 30 μm long [14,15]. This photocatalyst was easily dispersed in the photoreactor system and can be readily separated and reused owing to the long fibril morphology [14–16].

When nanofiber catalyst is integrated with a photocatalytic reactor, a multivariable system is created and may lead to a setback

* Corresponding author at: School of Earth and Environmental Sciences, The University of Adelaide, North Terrace Campus, Adelaide, SA 5005, Australia.
Tel.: +61 8 8303 7056; fax: +61 8 8303 6222.
E-mail address: bo.jin@adelaide.edu.au (B. Jin).

1385-8947/$ – see front matter © 2009 Elsevier B.V. All rights reserved.
doi:10.1016/j.cej.2009.10.017

towards process optimization and modelling. The conventional technique for optimization is bounded by the one-factor-at-a-time approach, while first principle model derivation with process validation has been a common practice associated with many studies on optimization and modelling of a photocatalytic process. Such techniques are fragile and time-consuming as they require rapid experimentations to validate and correlate the interactions between the operational factors involved [3,7,9,13,16]. Recently a number of statistical design of experiments (DOE) and data analysis techniques have been employed in various fields of process optimization [17–20]. These methods involve the use of statistical models to effectively design the experiments so as to reduce the number of experiments required while improving the results with a number of analysing techniques. Among the statistical methods, the Taguchi DOE method combined with response surface analysis (RSA) is recognised as a simple and reliable tool for a multivariable system [21–24]. The Taguchi DOE pre-determines the number of experiments required to cover the factors involved, while the RSA can effectively analyse the effects of several independent variables without any knowledge on the relationship between the objectives function and variables. The robustness of RSA includes building models, evaluating the effects of several factors and optimizing the process operating conditions to achieve desirable outcomes. While development and application of photocatalysts for water treatment have been intensively reported in the literature, use of combined DOE and RSA methodologies for optimization, identification of factors interaction and modelling of a photocatalytic system has been paid little attention.

This study was to apply the Taguchi DOE and RSA for identifying the optimum operation conditions for the degradation of Congo Red (CR). A recently developed H-titanate nanofiber catalyst (TNC) and a laboratory scale annular slurry photoreactor (ASP) system were employed in the study. Four key ASP operational factors of TNC loading, pH, aeration rate and initial CR concentration will be studied and the interaction between each chosen factors will be identified. A Taguchi DOE of L_9 $(3)^4$ array with 9 standard experiments will be used and the estimated average photocatalytic reaction rate from the batch kinetics data will be assigned as the response outputs for RSA interpretation. Finally, a statistical correlation that defines the chosen factors will be build by multiple linear regression technique for optimizing the photocatalytic process and identifying the factor interaction. A subsequent experiment validation was performed to test the accuracy of the model to predict the photocatalytic reaction rate.

2. Materials and methods

2.1. Materials

Congo Red ($C_{32}H_{22}N_6Na_2O_6S_2$, Colour Index 22120, Labchem Ajax Finechem, Australia), a secondary diazo was used as a surrogate indicator to simulate the industrial wastewater and to evaluate the photo-effectiveness of the TNC used in the APS system. Congo Red is a recalcitrant azo dye that is commonly found in industrial wastewater and thus considered suitable as an effectiveness measure, in terms of its chemical structure, molecular weight and diazo bonds. It has been involved in several photocatalysis studies including those using TiO_2 and hence is appropriate in making comparisons in this study. The chemical structure of the Congo Red is as shown in Fig. 1.

The *H-titanate nanofibers* were previously synthesized through a hydrothermal reaction between concentrated NaOH and TiO_2 and a post-synthesis ion exchange with HCl solution [14,15]. Specifically, 3 g of anatase particles (~325 meshes from Aldrich) was mixed with 80 mL of 10 M NaOH. The resultant suspensions were sonicated for 30 min and transferred into a PTFE container for autoclaving. The autoclave was maintained at hydrothermal temperature of 180 °C for 48 h. The precipitate (sodium titanate nanofibers) was recovered, washed with distilled water (to remove excess NaOH) and finally exchanged with H^+ (using a 0.1 M HCl solution) to produce hydrogen TNC. These products were repeatedly washed with distilled water until pH ~ 7 was reached. The hydrogen titanate product was dried at 80 °C for 12 h and then calcined at 700 °C for 3 h to yield anatase nanofibers. The TEM image of the single TNC fibril is shown in Fig. 2.

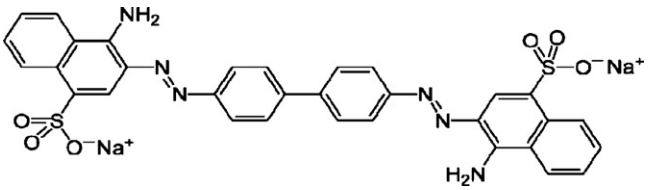

Fig. 1. Chemical structure of Congo Red (a secondary diazo dye).

2.2. Annular photocatalytic reactor system

A stainless steel-lined ASP was developed previously and used in this study [16]. The ASP was operated as a three-phase bubble column reactor, where the solid TNC were dispersed in the targeted water with the aid of compressed air. The lower end of the ASP was fabricated with a detachable conical bottom for free of reaction dead zone, making it easy for cleaning and maintenance. A 45 μm air sparger was fitted to the detachable conical bottom to provide homogeneous bubble distribution for agitation, mixing and sufficient dissolved oxygen for the photocatalytic reaction. The light configuration in the ASP was distinctively designed where additional light could be placed within the central quartz core. In this study, an UV light of 11 W (Davis Ultraviolet, Australia) was fitted annularly within the quartz thimble to prevent direct contact with the reaction fluid, while allowing optimal UV transmission for surface activation of the suspended TNC fibrils. Sampling during

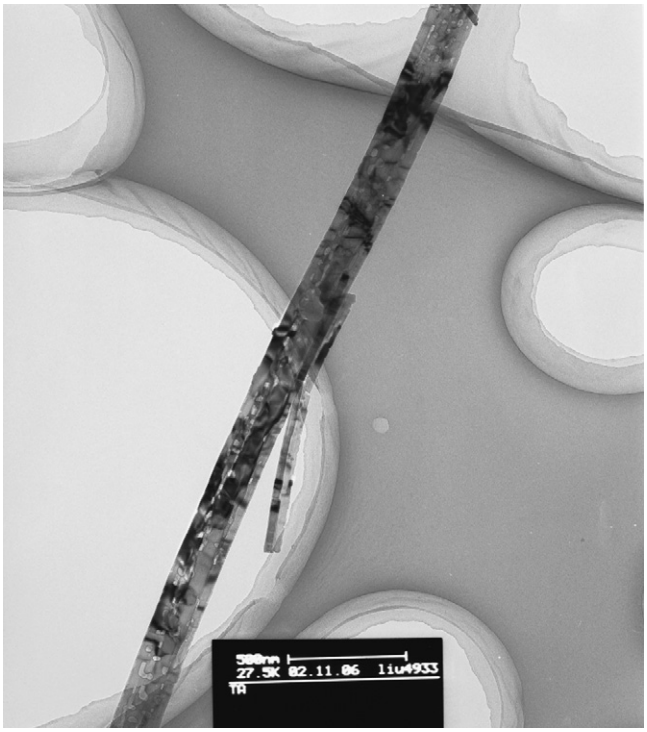

Fig. 2. The TEM image of a single TNC fibril.

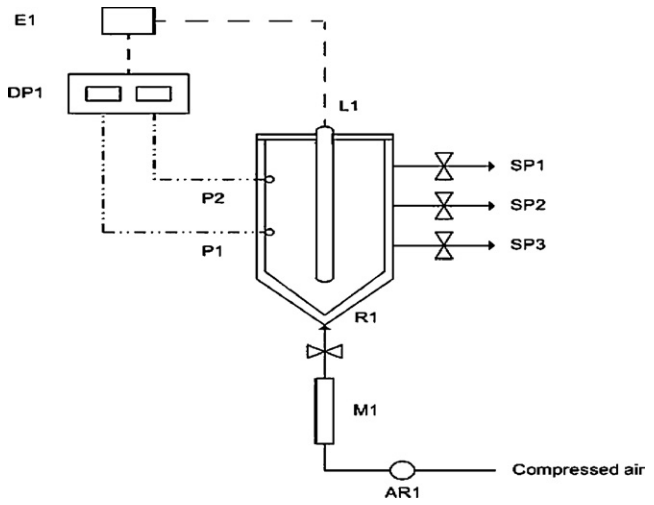

Fig. 3. Experimental setup for the annular photocatalytic reactor system: (E1) UV ballast, (L1) UV light, (DP1) monitoring meters, (P1) pH probes, (P2) dissolved oxygen probe, (SP1, 2, 3) sampling ports, (R1) photoreactor, (M1) air filter (AR1) compressed air regulation valve.

the batch kinetics study was facilitated by the four-level ports for effective fluid descending level sampling. Measurement probes and meters for in situ data logging of operational pH, dissolved oxygen (DO) and temperature (TPS, Australia) were connected to the reactor during investigation. A detailed design of the ASP and the whole experimental setup were shown in Fig. 3.

2.3. Experimental setup and analysis

The aqueous solution of CR was synthetically prepared to magnify its standard concentration in the natural occurrence of industrial wastewater. This allows the deficit to make up and represent other lower end molecular weight compounds. The aqueous CR solution was prepared with Nanopure water of 18.2 MΩ-cm to the designated concentration for each batch run. The initial pH of the CR solution was adjusted using 2 M HCl and 2 M NaOH and verified using a pH meter (TPS, Australia). The TNC were added and mixed thoroughly before charging into the ASP. A relatively low compressed air flow rate was allowed to run through the ASP to prevent rapid sedimentation when the CR-nanofibers mixtures were introduced. This mixture was remained in the ASP for a dark period of 30 min prior to the illumination of UV light. This was to ensure the uniformity in the batch kinetics data and to promote surface contact between the TNC and the CR. Subsequently, the samples from the ASP were collected at 1 h interval. The samples collected from the ASP were centrifuged at 5000 rpm for 10 min to separate the solid–liquid mixture so as to facilitate the decantation of supernatant for CR content analysis. The supernatant layer was then filtered using Millex VX filter (Millipore 0.45 um). All the filtered samples were subjected to UV–vis spectrophotometer (Helios Gamma, England) monochromatic measurement for its CR contents at 496.5 nm. This spectrophotometric measurement method has been previously verified to have a direct relationship between the CR content at 496.5 nm and its corresponding degree of mineralisation (i.e. in terms of its COD values) [16]. Each of the designated experimental runs was duplicated, with the average photocatalytic reaction rate taken for further statistical analysis.

2.4. Combined Taguchi and response surface analysis

Taguchi's orthogonal array (OA) is a statistical DOE of two-dimensional arrays of factors. This statistical DOE possess an interesting quality that by choosing any two columns, an even distribution of all pair-wise combinations for the studied factors will be obtained [23]. Compared to the conventional one-factor-at-a-time approach for optimization, the OA-based test combinations are dispersed uniformly throughout the study domain (i.e. only a small region was covered in the domain of conventional study) [23]. This allows the OA-based study combinations to be time-effective and enhances the identification of factor interactions when compared to the same number of studied factors in the conventional method [23]. Table 1 shows the L_9 $(3)^4$ orthogonal array designed for this study. From Table 1, it could be seen that the number of runs corresponds to the number of rows in the orthogonal array (i.e. number of generated study cases) while the number of the factors equates to the number of columns in the array [24]. The levels for the OA indicate the maximum number of values that can be taken by any single factor. The strength (i.e. $\text{Levels}^{\text{Strength}}$) shows the number of columns it can present each of the possibilities equally [24]. Thus the orthogonal array of L_9 $(3)^4$ in this study corresponds to L_{Runs} $(\text{Levels})^{\text{Factors}}$. The average photocatalytic reaction rate as estimated by Eq. (1) will be assigned as the response outputs for this Taguchi OA.

$$R_o = \frac{[CR]_o - [CR]_t}{t} \quad (1)$$

where R_o is the average photodegradation rate (R_o) of CR (mg dm^{-3} min^{-1}), [CR] is the CR concentration, t is the total reaction time (min) and the subscripts (o, t) corresponds to the initial reaction time and reaction time at t, respectively.

We used the RSA method to analyse and interpret the influence of the operation factors of TNC loading, pH, aeration rate and CR concentration on the R_o. Different RSA models will be evaluated on its fittingness in representing and modelling the DOE outcomes. A mathematical model, describing the correlation between the predicted R_o and the four operational factors will be developed. The polynomial model for the R_o was regressed with respect to the operational factors as in Eq. (2) [25–27]:

$$R_o = b_0 + \sum_{i=1}^{k} b_i X_i + \sum_{i=1}^{k} b_{ij} X_i^2 + \sum_{i_{i<j}}^{k} \sum_{j}^{k} b_{ij} X_i X_j \quad (2)$$

where R_o is the predicted response output of the photo-degradation rate, and i, j are linear, quadratic coefficients, respectively. The parameters of b and k are regression coefficient and the number of factors studied in the experiment, respectively, and X_i, X_j (I = 1, 4; j = 1, 4, $i \neq j$) represent the number of independent variables in the study. The accuracy and applicability for the estimated order of Eq. (2) polynomial model can be evaluated with the value of coefficient of determination R^2.

The analysis, evaluation and estimation of each coefficient were determined with Design Expert® Software Version 7.1.3. Statistical analyses and three-dimensional plots were obtained to determine both the interaction and optimal operational factors for the ASP. A subsequent experimentation was performed to validate the accuracy of the experimental value with model predicted value.

3. Results and discussions

3.1. Optimization of the operation conditions in the ASP

The effects of the four operational variables on the R_o in the ASP system were studied. To estimate the response outputs of R_o for the completion of Taguchi OA, the R_o was calculated according to Eq. (1). Table 1 shows the L_9 $(3)^4$ design of Taguchi OA and their standard factor combinations, together with the estimated R_o as the response outputs. These response outputs were then evaluated with different type of response surface models (i.e. mean, linear, 2 factors interaction (FI), quadratic and cubic) to compare

Table 1
Taguchi OA L_9 $(3)^4$ design for combinatorial optimization for the degradation of CR using H-titanate nanofibers photocatalysts.

Standard run	TNC loading ($g\,dm^{-3}$) (X_1)	pH (X_2)	Aeration rate ($dm^3\,min^{-1}$) (X_3)	Initial CR concentration ($mg\,dm^{-3}$) (X_4)	Response outputs ($mg\,dm^{-3}\,min^{-1}$)
1	2.00	3.00	2.50	20.00	0.0470
2	2.00	6.00	5.00	40.00	0.0957
3	2.00	9.00	7.50	60.00	0.1529
4	4.00	3.00	5.00	60.00	0.1174
5	4.00	6.00	7.50	20.00	0.0545
6	4.00	9.00	2.50	40.00	0.1432
7	6.00	3.00	7.50	40.00	0.0534
8	6.00	6.00	2.50	60.00	0.0944
9	6.00	9.00	5.00	20.00	0.1576

the appropriateness of each model. From the iteration procedures, it was found that the 2 factors interaction (FI) models with significant power transformation could adequately fit all the design points. Other order models exhibited a significant degree of lack of fit term, and thus inapplicable in this case. Most power transformation function can be described by a standard equation of:

$$\sigma = \mathrm{fn}(\mu^{\alpha}) \tag{3}$$

where fn is the functionalised model used, σ is the standard deviation, μ is the mean, α is the power, and λ is $(1-\alpha)$ in all cases. The initial value of λ in the standard equation will be $\lambda = 1$.

To yield the λ-value, the conventional Box–Cox (B–C) plot was used. This B–C plot enables a guideline for the selection of the correct power λ transformation [28]. Fig. 4 shows the B–C plot for the best λ-value when the starting $\lambda = 1$. From the B–C plot, the best lambda value was recommended in a range of -0.42 to 0.22 at a 95% confidence interval. These values were then investigated in different cases of $\lambda = -0.42$ and 0.22, respectively, for the accuracy in both adjusted and predicted R^2 values These values give a measure of the amount of variation about the mean (i.e. residual) as estimated by the model used. Also other conventional mathematical transformed models (i.e. square root, natural log and inverse square root) were evaluated simultaneously for their fittingness in representing the Taguchi OA response outputs. Table 2 lists the iteration outcomes for the suitability of each power order and mathematical transformed models. It was found that the natural log transformation of the response outputs as in Eq. (4) is the best mathematical model for the response outputs.

$$R'_o = \ln(R_o) \tag{4}$$

Table 2 shows that both the adjusted and predicted R^2 values varied in the order of 0.9994 and 0.9738, respectively. We use a multiple regression analysis methods to establish a natural logarithms response surface model, which is a statistical correlation that can represents the experiment data, as presented in Eq. (5):

$$\ln(R_o) = -2.38 - 0.041X_1 + 0.65X_2 + 0.34X_3 + 0.88X_4 + 0.81X_1X_2 + 0.47X_1X_3 - 0.13X_2X_3 \tag{5}$$

where $\ln(R_o)$ is the predicted response, which is the average photocatalytic degradation rate as estimated by Eq. (1). The independent variables of X_1, X_2, X_3 and X_4 are the coded representation for the test variables of the TNC loading, pH, aeration rate and CR concentration, respectively. Eq. (5) indicates that the positive coefficients of X_2, X_3, X_4, X_1X_2 and X_1X_3 have a constructive effect to increase the R_o, while the negative coefficients of X_1 and X_2X_3 affecting the reaction rate in a reverse manner.

Results from analysis of variance (ANOVA) on the established natural logarithmic transformed response surface model were summarized in Table 3. The Fisher's F-test was used to verify the statistical significance of Eq. (5). From the Fisher's F-test, the results show that the established model is statistically significant (i.e. ratio of mean square regression to mean square residual) with F-value of 2027.67 and a probability value (Prob > F) of 0.0171 [17–20,29]. This also evidenced by the determination coefficient (R^2) and the multiple correlation coefficients (R) [20]. In this case, the model predicted $R^2 = 0.9738$ indicates that the sample variation of 97.38% for the CR removal was attributed to the four independent variables, and only 2.62% of the total variation was unexplained by the established model. The adjusted $R^2 = 0.9994$ is also of statistical significance and dictates the correlation applicability of the model (Fig. 5). Fig. 5 shows the good agreement between the predicted and actual experimental values as evidenced by the points distributed along the diagonal line. This indicates that there was no significant violation of the model. This was further suggested by the lower value of the coefficient of variation (CV = 0.48%) [20]. Fig. 6 presents a plot of internally studentized residuals against the predicted response using the established natural logarithmic transformed response surface model. The irregular pattern of Taguchi OA experimental points in the plot without uniformity suggested that the variance of the original observation is constant [19]. This once proved that the established model is sufficient to estimate the photodegradation rate of CR in the studied span, as all the residuals are smaller than 5%.

A probability and Fisher's F-test was also conducted to check the significance of each of the coefficients and thus, the pattern of interaction between the test variables. Conventionally, the smaller the p-values ($p < 0.05$) indicate the higher the significance of the corresponding coefficient [17–20]. Table 3 shows the test estimation results for both the p-values and F-values of each chosen variables.

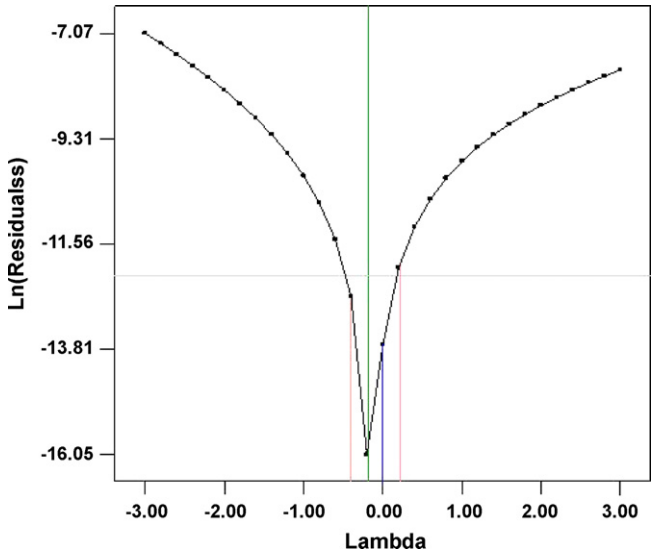

Fig. 4. Box–Cox plot for determination of the best power-transformed response surface model.

Table 2
Evaluation of different mathematical transformed models for response surface modelling of Taguchi response outputs.

Summary	$R_o^{\lambda=1.00}$	$R_o^{\lambda=-0.42}$	$R_o^{\lambda=0.22}$	$R_o^{\lambda=0.5}$	$\ln(R_o)$	$R_o^{\lambda=-0.5}$
Model *F*-value	39.39	673.66	343.90	114.56	2027.67	400.64
p-value (Prob > *F*)	0.1221	0.0297	0.0415	0.0718	0.0171	0.0384
Std. Dev.	7.451×10^{-3}	2.30×10^{-2}	3.55×10^{-3}	7.12×10^{-3}	1.10×10^{-2}	4.40×10^{-2}
Mean	0.10	2.77	0.60	0.31	-2.38	3.37
C.V.%	7.32	0.84	0.60	2.28	0.48	1.31
PRESS	0.0210	0.2000	0.0047	0.0190	0.0480	0.7200
R^2	0.9964	0.9998	0.9996	0.9988	0.9999	0.9996
Adjusted R^2	0.9711	0.9983	0.9967	0.9900	0.9994	0.9971
Predicted R^2	-0.3447	0.9211	0.8455	0.5366	0.9738	0.8674
S/N ratio	16.036	65.061	46.867	27.159	113.457	50.133
Residual	5.55×10^{-5}	5.46×10^{-4}	1.26×10^{-5}	5.06×10^{-5}	1.28×10^{-4}	1.94×10^{-3}

Table 3
ANOVA for natural logarithmic transformed response surface model for representation of Taguchi response outputs.

Source	Sum of squares (SS)	df	Mean square (MS)	*F*-value	*p*-value, Prob > *F*
Model	1.83	7	0.26	2027.67	0.0171
X_1-nanofibers loading	4.14×10^{-3}	1	4.41×10^{-3}	34.28	0.1077
X_2-pH	0.70	1	0.70	5449.63	0.0086
X_3-aeration rate	0.20	1	0.20	1551.09	0.0162
X_4-initial [CR]	0.66	1	0.66	5150.99	0.0089
X_1X_2	0.38	1	0.38	2961.87	0.0117
X_1X_3	0.13	1	0.13	1010.02	0.0200
X_1X_4	0.00	0	0.00	0.00	0.0000
X_2X_3	0.02	1	0.02	154.61	0.0511
X_2X_4	0.00	0	0.00	0.00	0.0000
X_3X_4	0.00	0	0.00	0.00	0.0000
Residual	1.29×10^{-4}	1	1.29×10^{-4}		
Total	1.83	8			

These results suggest that the effects of pH are the most significant on the overall photocatalytic reaction rate in the ASP (*p*-value of 0.086), followed by initial CR concentration and aeration rate with *p*-values of 0.089 and 0.0162, respectively. The nanofibers loading in the ASP is the least significant variables that affect the photocatalytic reaction rate with highest *p*-value of 0.1077. However it must be noted that the effects of nanofibers loading (X_1) become profound when the interactive factors take into account with pH (X_2) and aeration rate (X_3) as indicated by the positive X_1X_2 and X_1X_3 terms in Eq. (5). The initial CR concentration (X_4) is an independent variable in this case and thus, the optimal photocatalytic rate can be attained after optimizing the variables of X_1, X_2 and X_3.

The three-dimensional (3D) response surface plots as presented in Fig. 7 are graphical representations of the established regression equation (Eq. (5)) to achieve better understanding for the interactions between variables and to determine the optimum level of each variable for maximum photocatalytic oxidation rate of CR in the ASP system [19]. For the 6 possible two-variable combination interaction, three pairs was determined as the prominent contributors (sum of squares > 0) to the operational conditions in the ASP, which is the X_1X_2, X_1X_3 and X_2X_3 with their corresponding low *p*-values. The other three combinations have aliased the other terms in the model used and thus were not uniquely estimated for their *p*-values. From Fig. 7a and b, it was found that the nanofibers loadings (X_1) have positive synergistic effects when being coupled with

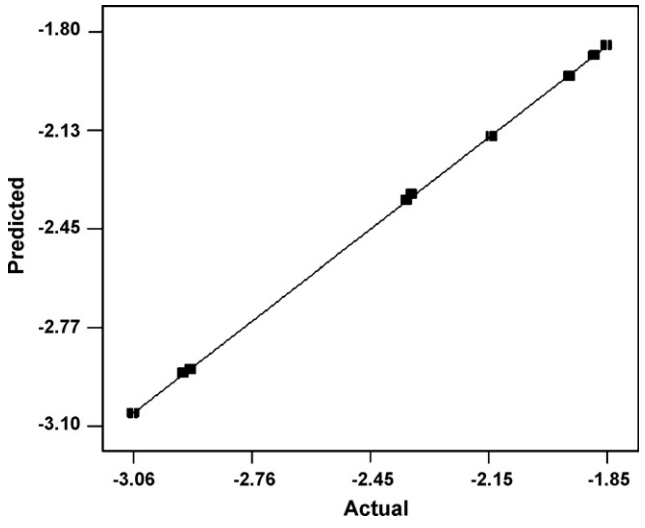

Fig. 5. Plot of predicted versus actual value of response outputs (i.e. predicted using the developed natural logarithmic modified response surface model).

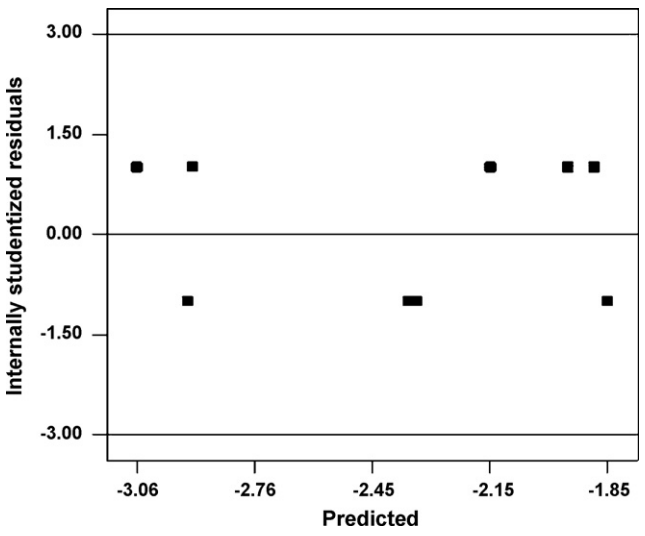

Fig. 6. Plot of internally studentized residuals against model predicted value.

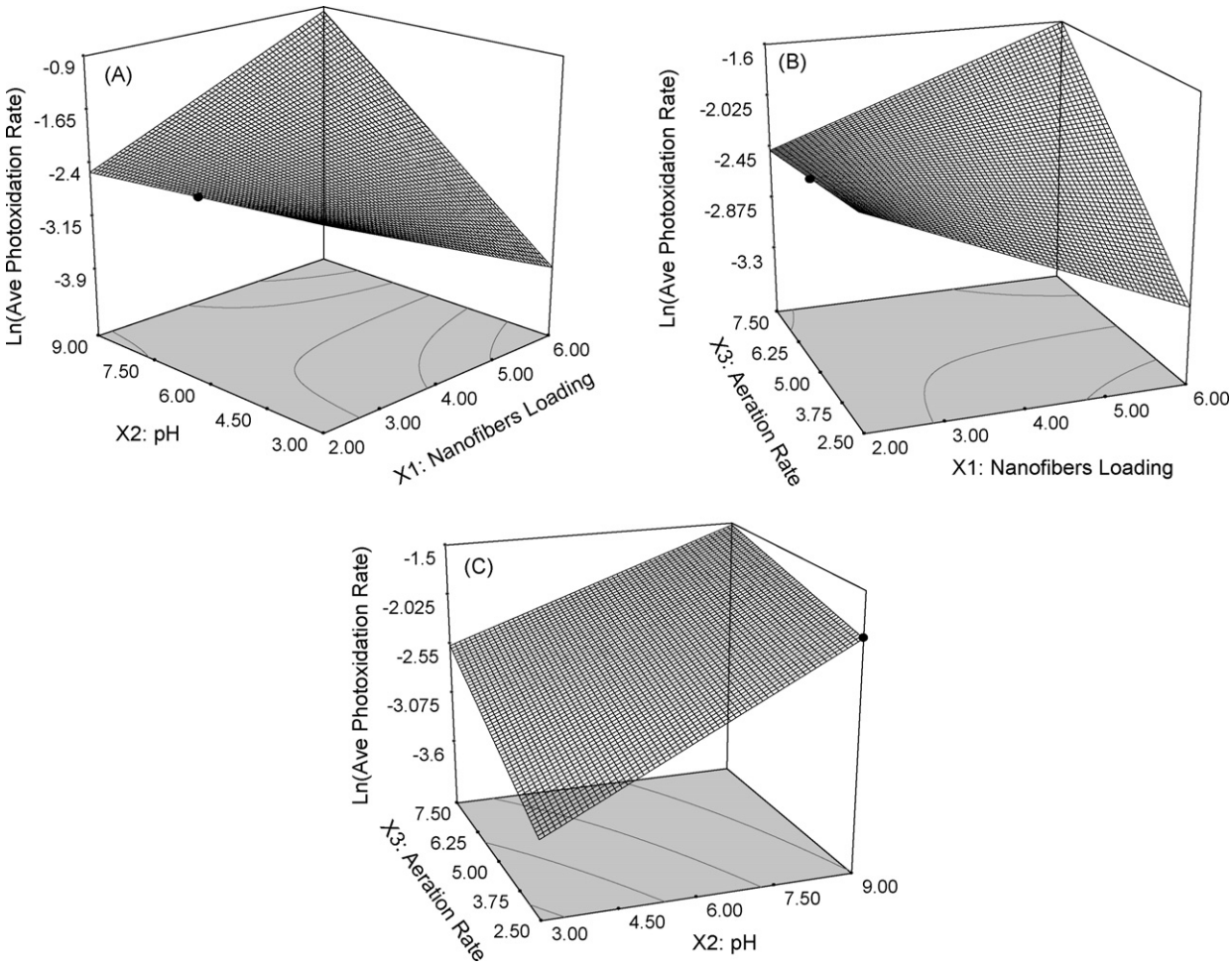

Fig. 7. 3D response surface plots for the photo-oxidation of CR in ASP using H-titanate nanofibers photocatalyst showing the interaction between (A) TNC loading and pH; (B) TNC loading and aeration rate; and (C) pH and aeration rate.

the pH (X_2) and aeration rate (X_3), respectively. This was evidenced from the positive terms in Eq. (5) and also the convex response surfaces that indicate well-defined optimum variables. However it must be emphasized that the singular effect of nanofibers loading on its photocatalytic oxidation rate of CR has a negative impact as observed in Eq. (5). This means that an increase in the singular nanofibers loadings variable in the ASP system will have an adverse effect on the overall photocatalytic reaction rate. Similar positive synergistic effect was observed when the nanofibers loading was coupled with the amount of compressed air delivered into the ASP system (Fig. 7b). As for the interaction between pH (X_2) and aeration rate (X_3), a rather symmetric and flat response surface was observed (Fig. 7c) near the optimum point and this point will be stagnant and not subjected to much variations. However this pair of X_2X_3 variables combination is not statistically significant in terms of their p-values and undesirable negative terms in Eq. (3). With the aid of Design Expert® software for response surface optimization, in terms of the maximal photocatalytic reaction rate of CR in the ASP, 39 combinations were attained.

3.2. Interactions between the operational variables in the ASP system

Optimization of the operational factors in a photocatalytic reactor system has been reported in previous studies [3,7,9,13]. The effects of the operational factors, mainly the TNC loading, pH, aeration rate and initial CR concentration, on the photocatalytic degradation performance were investigated using the conventional one-factor-at-a-time approach [16]. However most of these studies adopted such conventional optimization strategy, where the knowledge of the interaction between the operation factors was often neglected. This knowledge is important, particularly for optimizing the performance and minimising the operation cost for an industrial photocatalytic treatment processes. In this section, the interactions between the operational factors as determined in Section 3.1 will be rationalised and discussed in details.

The interaction between the TNC loading (X_1) and pH (X_2) is the dominant factor combination ($p = 0.0117$). Since the X_1X_2 interaction has a positive term in Eq. (5), this does not indicate that increasing both values simultaneously will contribute to a high photo-degradation rate. This was proven by the occurrence of negative term for the TNC loading (X_1) as in Eq. (5). In most of the photocatalytic studies, the amount of photocatalysts added as a suspension in a fixed reaction volume will eventually reach a saturation level, where an excessive amount of photocatalysts will compete for light photons and radially attenuating the light intensity [3,7,9]. Thus the interaction between the X_1 and X_2 is proposed in such a way where the singular effects of X_1 and X_2 counterbalance each other to achieve optimum photoactivity, as represented by the interactive X_1X_2 term. As reported in many previous studies, the nature of the TiO_2 surface exhibits zwitterionic properties as being exposed to different pH conditions [3,7,9,13,16]. At a pH lower than the point of zero charge (PZC) of TiO_2, the TiO_2 surface will be positively charged and attracts oppositely charged ions to

the vicinity of its surface for photocatalytic reaction [7,9]. Since dissolved CR is an anionic molecules, it is anticipated that at pH < PZC (TiO_2) and ascending nanofibers concentration beyond the ASP saturation level, the maximum photocatalytic reaction rate will be attained. From Fig. 7a, other possibility is that at pH > PZC (TiO_2) (i.e. with increasing electrostatic repulsion between the nanofibers and CR), these electrostatic effect can be compensated by higher nanofibers loading to increase the possibility of surface contact and hence, counterbalance the photocatalytic reaction rate [30].

Similar counterbalance interactive term was also observed in the nanofibers loading (X_1) with aeration rate (X_3) used in the ASP system (Fig. 7b), owing to the adversity of X_1 variable in Eq. (5). The interactive combination of low nanofibers loading (up to saturation level) with high aeration rate (above 5 $dm^3\ min^{-1}$) can yield an optimal reaction rate owing to a higher degree of homogeneous dispersion and mixing. At higher nanofibers loading with lower aeration rate (2.5 $dm^3\ min^{-1}$), an irregular mixing pattern and rapid sedimentation of the nanofibers that blocked the bubble sparger plate was observed at the end of each batch run. Chin et al. [9] observed that at an ascending aeration rate, the size of the bubble formed will also increase and further creates a shielding effect (bubble clouds) against the efficient distribution of light photons in the reactor. This will further weight on the effective attenuation of light photons within the reactor when the nanofibers loading was well above the saturation level.

As for the interactive term between the effects of pH (X_2) and the aeration rate (X_3) in Eq. (5), the interaction outcomes were different from the previously discussed X_1X_2 and X_1X_3 terms (Fig. 7c). This is owing to the critical nature of this X_2X_3 term in the regression equation (Eq. (5)) that will eventually lowered the overall photocatalytic reaction rate. Although it was known that such term was detrimental, the optimum level for this variable pair should be well understood in order to minimise its unfavourable effect. Fernande-Ibanez et al. [31] discussed that to reduce the aggregation between the TiO_2 particles used; the operating pH should be well maintained near the PZC (TiO_2). This is to reduce the possible surface interaction between the polar molecules at pH distant from the PZC (TiO_2), which will reduce the specific surface area due to particles aggregation. In addition, low aeration rate (2.5 $dm^3\ min^{-1}$) should be avoided from coupling with pH distant from PZC (TiO_2), as this will further promotes the formation of large TiO_2 clumps during the batch reaction. From the previous study, it was observed that best possible combination between these variables of X_2 and X_3, should be attained at pH ~ PZC (TiO_2) and high aeration rate in the ASP (5 $dm^3\ min^{-1}$ and above). This will minimise the possible aggregation of TiO_2 nanofibers with rapid bubbling to disintegrate the large TiO_2 clumps formation and further promotes homogeneous dispersion of nanofibers for maximum photo-efficiency. Chin et al. [9] also observed and reported similar findings at high aeration rates, where the bubbling produced greater shear rates to prevent TiO_2 agglomeration that leads to higher surface area for photocatalytic reaction.

3.3. Verification of the established model

As reported in Section 3.1, a maximum photocatalytic degradation rate in the ASP system can be achieved with the optimal combinations via 39 different permutations of the operation variables. The optimum photocatalytic degradation rate was 0.1576 mg $dm^{-3}\ min^{-1}$ at a particular combination; nanofiber loading of 6 g dm^{-3}, pH 9, aeration rate of 5 $dm^3\ min^{-1}$ and 20 mg dm^{-3} of the initial CR concentration. All the optimal values were located within the experimental span and varied around the centre points to a limited extent. Subsequently, a verification experiment on the chosen variable combination in achieving the reaction rate of 0.1576 mg $dm^{-3}\ min^{-1}$ was carried out in the ASP system. The average photocatalytic degradation rate was found to be 0.1563 ± 0.0282 mg $dm^{-3}\ min^{-1}$. This showed that the established regression model for the current experimental span was highly robust in predicting the experimental outcomes. Further efforts can be dedicated, when expanding the current model to incorporate different water quality by introducing a fractional corrective factor. This can be realised by taking the current model prediction as the base case.

4. Conclusion

This study showed the development and application of statistical design of experiments and response surface analysis for determining the optimal operation variables for optimizing the photocatalytic degradation process using H-titanate nanofiber catalyst. The results generated from the statistical analysis and model evaluation revealed that the DOE and RSA methods can be effectively adopted to optimize operation variables and to determine their interactions in the ASP system, which demonstrated an overall advantage over the conventional one-factor-at-a-time method. In combination with the Taguchi DOE, a time-effective statistical approach was developed in solving the multivariables associated with the TiO_2 photocatalytic water treatment system. In addition, the developed regression model could be effectively used as a modelling and design tool for scaling up the ASP system to a commercial scale process. This was considered as an innovative and robust approach for system modelling over the conventional first principle derivation model that requires rapid parameters validation. Subsequent work should be expanded to build a more realistic model by incorporating different water qualities, by taking the current result as the base case.

Nomenclature

ANOVA	analysis of variance
ASP	annular slurry photoreactor
Ave	average
b	regression coefficient
B–C	Box–Cox
COD	chemical oxygen demand
CR	Congo red
CV	coefficient of variation
df	degree of freedom
DO	dissolved oxygen
DOE	design of experiment
FI	factor interaction
fn	function
HCl	hydrochloric acid
H_2O_2	hydrogen peroxide
Ln	natural logarithmic
$L_9(3)^4$	Taguchi orthogonal array
M	molar (mol L^{-1})
MS	mean square
NaOH	sodium hydroxide
$O_2^{\bullet -}$	superoxide radical
OA	orthogonal array
$OH^{\bullet}$	hydroxyl radical
PTFE	polytetrafluoroethylene
PZC	point of zero charge
R_o	average photodegradation rate (mg $dm^{-3}\ min^{-1}$)
R'_o	natural log-transformed rate output
R^2	correlation coefficient
R&D	research and development

rpm revolution per minute
RSA response surface analysis
S/N signal-to-noise ratio
SS sum of squares
Std. Dev. standard deviation
t total reaction time (min)
TEM transmission electron microscopy
TiO_2 titanium dioxide
TNC H-titanate nanofiber catalyst
UV ultraviolet
X independent variable

Subscripts
o initial reaction time, $t = 0$
t reaction time, t
i linear coefficient
j quadratic coefficient
k number of factors

Greek symbols
σ standard deviation
μ mean
α power
λ 1 − power

Acknowledgement

The authors would like to thank their Honour students Ruofei Yee and Zhongde Lim for their technical assistances. This work was funded by the Australian Research Council Linkage Grant (LP0562153) and the Australian Water Quality Centre, SA Water Corporation through the Water Environmental Biotechnology Laboratory (WEBL) at the University of Adelaide.

References

[1] S. Mozia, M. Tomaszewska, A.W. Morawski, Photodegradation of azo dye Acid Red 18 in a quartz labyrinth flow reactor with immobilized TiO_2 bed, Dyes Pigments 75 (2007) 60–66.
[2] L. Rizzo, J. Koch, M.A. Anderson, Removal of methylene blue in a photocatalytic reactor using polymethylmethacrylate supported TiO_2 nanofilm, Desalination 211 (2007) 1–9.
[3] I.J. Ochuma, R.P. Fishwick, J. Wood, J.M. Winterbottom, Optimisation of degradation conditions of 1,8-diazabicyclo[5.4.0]undec-7-ene in water and reaction kinetics analysis using a cocurrent downflow contactor photocatalytic reactor, Appl. Catal. B: Environ. 73 (2007) 259–268.
[4] K. Pirkanniemi, M. Sillanpaa, Heterogeneous water phase catalysis as an environmental application: a review, Chemosphere 48 (2002) 1047–1060.
[5] D. Bahnemann, Photocatalytic water treatment: solar energy applications, Sol. Energy 77 (2004) 445–459.
[6] U.I. Gaya, A.H. Abdullah, Heterogeneous photocatalytic degradation of organic contaminants over titanium dioxide: a review of fundamentals, progress and problems, J. Photochem. Photobiol. C: Photochem. Rev. 9 (2008) 1–12.
[7] A.P. Toor, A. Verma, C.K. Jotshi, P.K. Bajpai, V. Singh, Photocatalytic degradation of Direct Yellow 12 dye using UV/TiO_2 in a shallow pond slurry reactor, Dyes Pigments 68 (2006) 53–60.
[8] A. Fujishima, K.K. Honda, Photolysis-decomposition of water at surface of an irradiated semiconduction, Nature 238 (1972) 37.
[9] S.S. Chin, T.M. Lim, K. Chiang, A.G. Fane, Factors affecting the performance of a low-pressure submerged membrane photocatalytic reactor, Chem. Eng. J. 130 (2007) 53–63.
[10] M.N. Chong, V. Vimonses, S. Lei, B. Jin, C. Saint, C. Chow, Synthesis and characterisation of novel titania impregnated kaolinite nano-photocatalyst, Micropor. Mesopor. Mater. 117 (2009) 233–242.
[11] J.S. Jang, W. Li, S.H. Oh, J.S. Lee, Fabrication of CdS/TiO_2 nano-bulk composite photocatalysts for hydrogen production from aqueous H_2S solution under visible light, Chem. Phys. Lett. 425 (2006) 278–282.
[12] R.L. Pozzo, J.L. Giombi, M.A. Baltanas, A.E. Cassano, The performance in a fluidized bed reactor of photocatalysts immobilized onto inert supports, Catal. Today 62 (2000) 175–187.
[13] A. Bhargava, M.F. Kabir, E. Vaisman, C.H. Langford, A. Kantzas, Novel technique to characterize the hydrodynamics and analyze the performance of a fluidized-bed photocatalytic reactor for wastewater treatment, Ind. Eng. Chem. Res. 43 (2004) 980–989.
[14] H. Zhu, X. Gao, Y. Lan, D. Song, Y. Xi, J. Zhao, Hydrogen titanate nanofibers covered with anatase nanocrystals: a delicate structure achieved by the wet chemistry reaction of the titanate nanofibers, J. Am. Chem. Soc. Commun. 126 (2004) 8380–8381.
[15] H.Y. Zhu, Y. Lan, X.P. Gao, S.P. Ringer, Z.F. Zheng, D.Y. Song, J.C. Zhao, Phase transition between nanostructures of titanate and titanium dioxides via simple wet-chemical reactions, J. Am. Chem. Soc. 127 (2005) 6730–6736.
[16] M.N. Chong, B. Jin, H.Y. Zhu, C. Chow, C. Saint, Application of H-titanate nanofibers for degradation of Congo Red in an annular slurry photoreactor, Chem. Eng. J. 150 (2009) 49–54.
[17] L. Levin, C. Herrmann, V.L. Papinutti, Optimization of lignocellulolytic enzyme production by the white-rot fungus *Trametes trogii* in solid-state fermentation using response surface methodology, Biochem. Eng. J 39 (2008) 207–214.
[18] X. Chen, W. Du, D. Liu, Response surface optimization of biocatalytic biodiesel production with acid oil, Biochem. Eng. J. 40 (2008) 423–429.
[19] L. Yu, T. Lei, X. Ren, X. Pei, Y. Feng, Response surface optimization of l-(+)-lactic acid production using corn steep liquor as an alternative nitrogen source by *Lactobacillus rhamnosus* CGMCC 1466, Biochem. Eng. J 39 (2008) 496–502.
[20] Q. Wang, H. Ma, W. Xu, L. Gong, W. Zhang, D. Zou, Ethanol production from kitchen garbage using response surface methodology, Biochem. Eng. J. 39 (2008) 604–610.
[21] W. Charteris, Taguchi's system of experimental design and data analysis: a quality engineering technology for the food industry, J. Soc. Dairy Technol. 45 (1992) 33–49.
[22] K.D. Kim, S.H. Kim, H.T. Kim, Applying the Taguchi method to the optimization for the synthesis of TiO_2 nanoparticles by hydrolysis of TEOT in micelles, Colloids Surf. A: Physicochem. Eng. Aspects 254 (2005) 99–105.
[23] G. Taguchi, System of Experimental Design Volumes 1 and 2, UNIPUB Krauss International, New York, 1987.
[24] Z. Li, O.P. Malik, An orthogonal test approach based control parameter optimizationand its application to a hydro-turbine governor, IEEE Trans. Energy Conver. 12 (1997) 388–393.
[25] R.D. Cook, Residuals and Influence in Regression, Chapman and Hall, New York, 1982.
[26] E. Sayan, M. Bayramoglu, Statistical modeling of sulfuric acid leaching of TiO_2 from red mud, Hydrometallurgy 57 (2000) 181–186.
[27] A.F. Caliman, C. Cojocaru, A. Antoniadis, I. Poulios, Optimized photocatalytic degradation of Alcian Blue 8 GX in the presence of TiO_2 suspensions, J. Hazard. Mater. 144 (2007) 265–273.
[28] G.E.P. Box, D.R. Cox, An analysis of transformation (with discussion), J. R. Stat. Soc. B26 (1964) 211–252.
[29] Y.S. Song, D.Y. Lee, B.Y. Kim, Effect of glass frit addition on corrosion resistance of Ti/TiO_2/IrO_2–RuO_2 films, Mater. Lett. 58 (2004) 817–823.
[30] R.A. Burns, J.C. Crittenden, D.W. Hand, V.H. Selzer, L.L. Sutter, S.R. Salman, Effect of inorganic ions in heterogeneous photocatalysis of TCE, J. Environ. Eng. 125 (1999) 77–85.
[31] P. Fernande-Ibanez, J. Blanco, S. Malato, F.J. Nieves, Application of the colloidal stability of TiO_2 particles for recovery and reuse in solar photocatalysis, Water Res. 37 (2003) 3180–3188.